Geology, Geophysics & Environment 2024, vol. 50 (2): 155–174

Ash admixtures formed during the loss on ignition (LOI) procedure and their impact on laser textural analysis results

Dmitry Tsvirko[1], Wojciech Tołoczko[2], Piotr Kittel[3]

[1] *University of Lodz, Doctoral School of Exact and Natural Sciences, Łódź, Poland,*
e-mail: dzmitry.tsvirka@edu.uni.lodz.pl (corresponding author), ORCID ID: 0000-0002-5913-050X
[2] *University of Lodz, Faculty of Geographical Sciences, Department of Physical Geography, Łódź, Poland,*
e-mail: wojciech.toloczko@geo.uni.lodz.pl, ORCID ID: 0000-0001-5441-4418
[3] *University of Lodz, Faculty of Geographical Sciences, Department of Geology and Geomorphology, Łódź, Poland,*
e-mail: piotr.kittel@geo.uni.lodz.pl, ORCID ID: 0000-0001-6987-7968

Received: 2 August 2023; accepted: 29 April 2024; first published online: 7 June 2024

Abstract: We present an experimental study that explores the feasibility of using the ash from biogenic deposits for laser textural analysis. The results have demonstrated that conducting ash textural analysis without prior chemical treatment can lead to unreliable results. Among other things, this is due to the "contamination" of the ash with aggregates formed by metal oxides and carbonates during ignition (LOI_{550} procedure) in a muffle furnace. Metal oxides and carbonates can create aggregates with silt and clay grains. As a result, the material coarsens, mainly to very coarse and coarse silt fractions. It is illustrated that the ash after LOI_{550} has been contaminated with oxides and carbonates of iron (Fe), potassium (K), magnesium (Mg), calcium (Ca), manganese (Mn), sodium (Na), zinc (Zn), lead (Pb) and copper (Cu). Thus, we suggest a method of using 10% HCl to purify the ash from metal oxides and carbonates (so-called ash purification procedure or APP). The analysis in this paper focuses on the grain size composition of ash, both untreated and HCl-treated. The obtained results have been compared and discussed in detail.

Keywords: loss on ignition, biogenic deposits ash, laser textural analysis, ash purification procedure (APP), metal oxides and carbonates

INTRODUCTION

Peat, gyttja, and other biogenic deposits consist of a combination of organic matter (organic component), primarily derived from plant remains, and mineral particles of different origin (mineral component). In river valleys, the main sources of the influx of mineral particles into peat and gyttja deposits are floods, aeolian deposition, and slope processes. Textural (grain size distribution) analysis of the mineral component of biogenic deposits is highly valuable. It can be useful for tracking changes in deposition processes and the origin of mineral fractions, which is helpful for palaeogeographical reconstructions or identifying lithological boundaries. The primary issue revolves around the challenge of isolating the mineral portion of biogenic deposits from their organic counterpart. A feasible option could be utilizing ignition in a muffle furnace to remove the organic substances from deposits. Currently, the loss on ignition (LOI_{550}) method is extensively applied, and the resulting ash can be used for textural analysis. In some studies, researchers have already utilized the

untreated ash obtained after ignition for textural analysis (Kittel et al. 2014, 2016, 2020, Żarczyński et al. 2019).

Ignition in a muffle furnace at a temperature of 950°C (or 925°C) can also be used to remove organic matter, as well as calcium carbonate ($CaCO_3$) from sediments (Heiri et al. 2001). Another method for removing organic matter is boiling in hydrogen peroxide H_2O_2 (Mikutta et al. 2005). However, our research is focused only on the study of the ash obtained after ignition at a temperature of 550°C – LOI_{550}.

This paper demonstrates that the ash remaining after LOI_{550} procedure differs from the mineral component of biogenic deposits. Additionally, the LOI_{550} readings do not accurately indicate the amount of organic matter present in the examined deposits. After the furnace, the ash becomes filled with metal oxides and carbonates that are produced during ignition at 550°C. This leads to contamination of the mineral component of biogenic deposits and to a decrease in the actual amount of organic matter present in the final results. During ignition at 550°C, the organic component of biogenic deposits is not entirely removed from the samples. Instead, the released carbon dioxide (CO_2) reacts with metals to form metal carbonates. The formation of new compounds that contaminate and add weight to the resulting ash also involves ambient oxygen (O_2). An additional problem is formation of aggregates of these newly established oxides and carbonates with silt and clay grains.

Accordingly, our study has the following objectives:

- Create a procedure for purifying the ash from secondary metal oxides and carbonates (for instance, Fe_2O_3, K_2CO_3, $MgCO_3$ and $CaCO_3$) that are produced during ignition at a temperature of 550°C.
- Perform a spectral analysis with SPEKOL11 equipment on the HCl acid solutions obtained during the ash purification procedure (APP). This will help estimate the amount of iron and its oxides present in the studied ash. Determine other metals present in the acid solutions using the atomic absorption spectroscopy (AAS) method.
- Conduct a laser textural analysis with a Malvern Panalytical Mastersizer 3000 equipment on the ash purified from metal oxides and carbonates (the HCl-treated ash), as well as on the ash that has not been purified from these compounds (the untreated ash) and compare the results.

Some of the findings from this study have been previously published in conference proceedings by Tsvirko et al. (2022a, 2022b). This research revises and adds to our previous perspectives as presented in our past publications. In particular, it was not previously taken into account that iron carbonates $FeCO_3$ and $Fe_2(CO_3)_3$ decompose during the heating process to 550°C, and iron carbonates are not preserved in the ash after a muffle furnace (Kissinger et al. 1956). In our previous publications, we called the ash purification procedure (APP) as the HCl cleaning procedure or HCLP (Tsvirko et al. 2022a, 2022b, Tsvirko 2023).

MATERIALS AND METHODS

Fifteen samples (nos. 3–15 and 31, 32) from the core PKK-1-2 (Figs. 1, 2, Table 2) were used for analyses (see also Table S1 and Figure S1 in the online supplementary material (OSM)). The core was taken from a fen located near the channel of the Yaselda River in southern Belarus (Tsvirko et al. 2021a). The studied deposits were characterized by different amounts of organic matter: biogenic deposits (coarse detritus gyttja, black/brown telmatic peat, fen peat according to Markowski (1980) and Tobolski (2021) classifications), and sandy deposits with a small amount of organic matter (Fig. 3). The analysis of plant macrofossils was used to identify the origin of these geological sediment layers. Coarse detritus gyttja was characterized by a predominance of macroremains of fully submerged plants and plants with floating leaves (*Chara*, *Potamogeton*, *Nuphar*, *Nymphaea*, *Stratiotes aloides*, etc.). Telmatic peat was characterized by a predominance of macroremains of semi-submerged and nearshore vegetation (*Typha*, *Alisma plantago aquatica*, *Sagittaria sagittifolia*, *Juncus*, *Mentha longifolia*, Poaceae, etc.), with a still significant admixture of remains of fully submerged plants and plants with floating leaves (*Chara*, *Potamogeton*, *Lemna*, *Salvinia natans*, *Stratiotes aloides*, etc.).

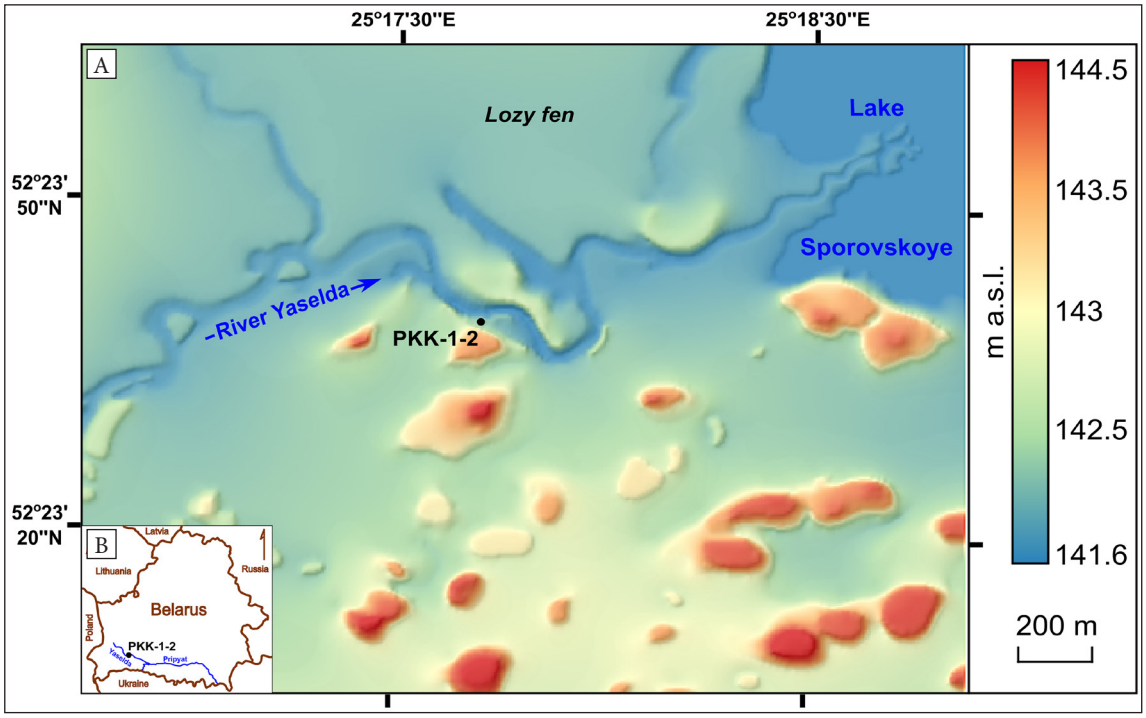

Fig. 1. *Location of the studied PKK-1-2 core in the basin of the Yaselda River and Lake Sporovskoye (A) in southern Belarus (B) (Tsvirko et al. 2021b, Tsvirko 2023)*

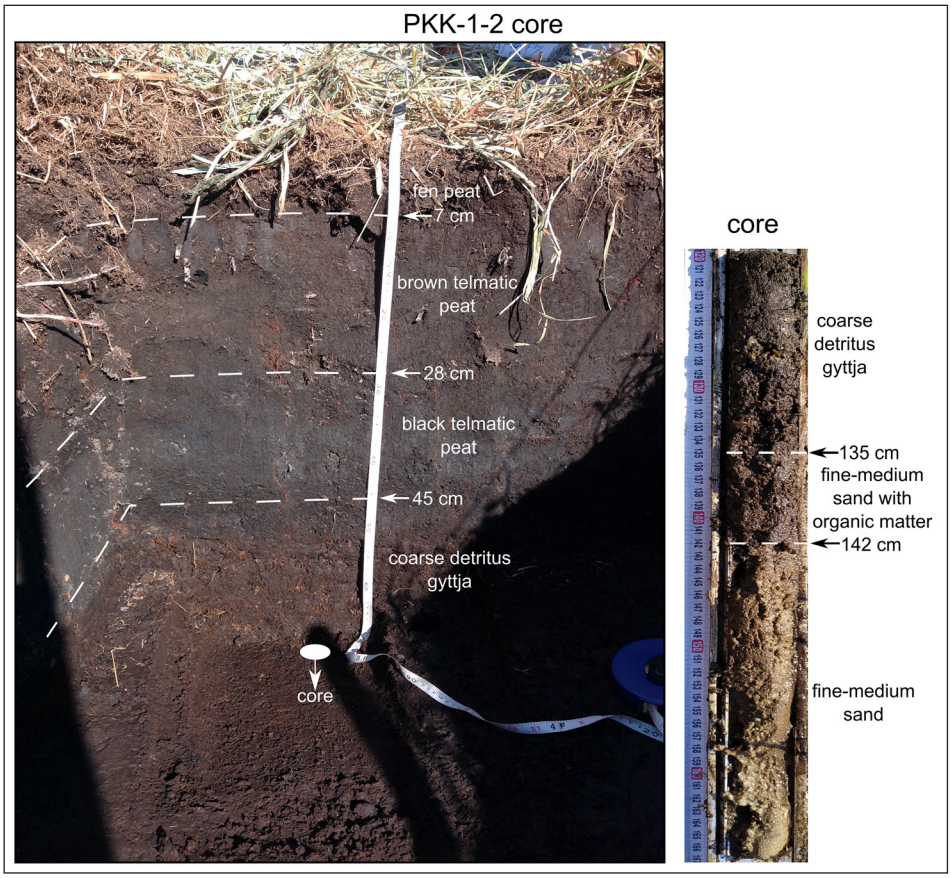

Fig. 2. *Deposits of the PKK-1-2 core (52°23'38.448"N 25°17'35.545"E). The photos represent only the part of the studied deposits with marked lithological boundaries (photos by D. Tsvirko, August 2020)*

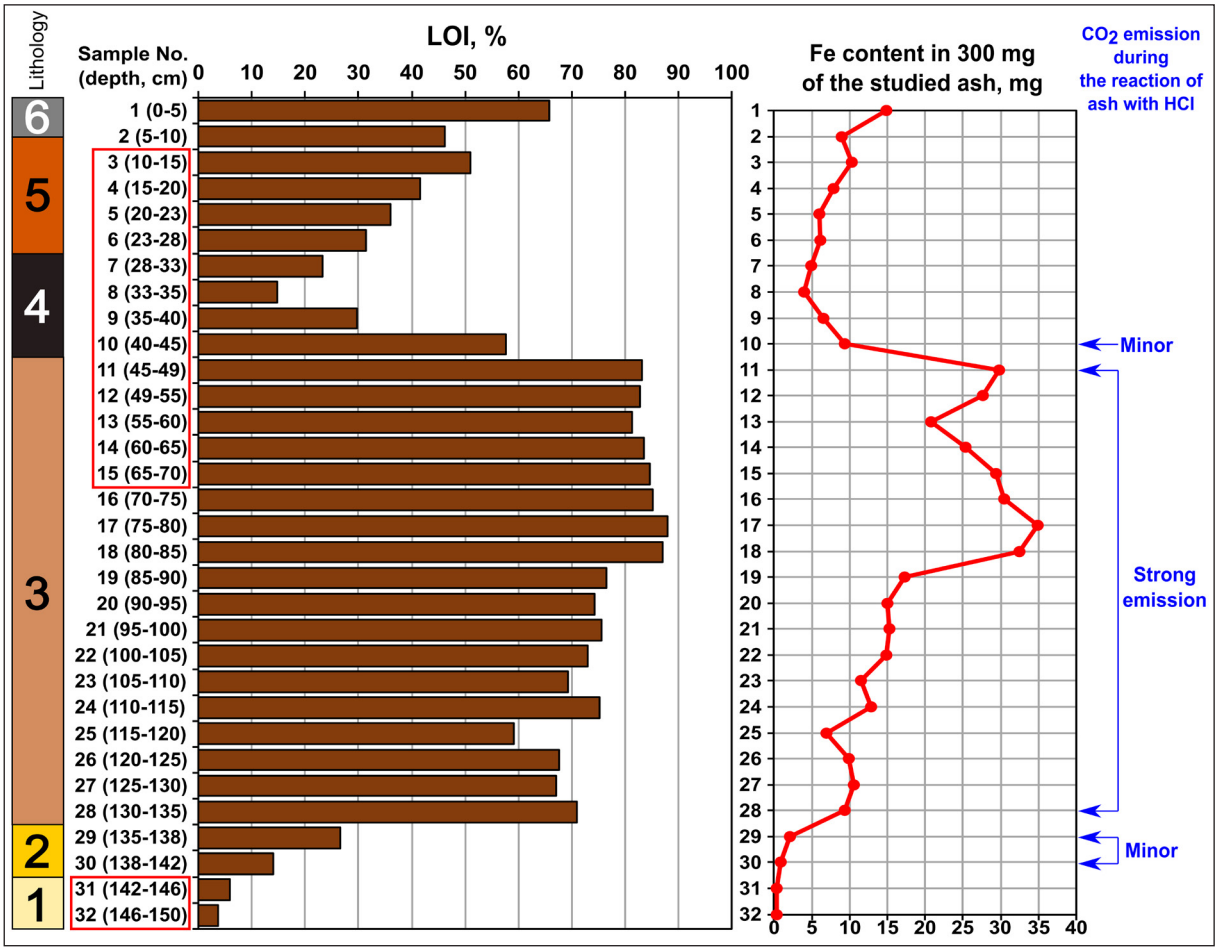

Fig. 3. *Core PKK-1-2 with LOI_{550} values, the amount of iron in 300 mg of ash (based on SPEKOL11 analysis and on initial masses of ash used for APP at room temperature), and the designation of samples that had CO_2 emission during the reaction of ash with HCl. The main studied samples are marked with red squares. Lithology: 1 – fine-medium sand, 2 – fine-medium sand with organic matter, 3 – coarse detritus gyttja, 4 – black telmatic peat, 5 – brown telmatic peat, 6 – fen peat*

Also, the studied core PKK-1-2 can be characterized as an organic peat soil, without visible gley features, but with iron precipitation associated with groundwater level fluctuations and visible in geochemical analysis (Fig. 3).

The samples were dried at 50°C (24 hours) and carefully ground in a porcelain mortar. Before ignition, the samples were dried at a temperature of 105°C (1 hour), and the empty crucibles at 550°C (1 hour) to remove any remaining moisture. The samples were then subjected to combustion in a muffle furnace at 550°C for 8 hours. To determine the LOI_{550} values, the weight of dry samples and dry crucibles were measured both before and after ignition, following the procedure outlined by Dean (1974) and Heiri et al. (2001). It has to be noted that the weight of the dry samples and crucibles was measured immediately after drying them (at 105°C), or after the muffle furnace cooled to 100°C (i.e. without storage in the laboratory). Desiccators were not used in this study, but we strongly recommend them. The initial results of loss on ignition (LOI_{550}) are shown in Table 2 and Figure 3.

After the LOI_{550} process, the ash was thoroughly homogenized and split into two subsamples. Subsample one was analyzed for its textural features (grain size distribution) using laser particle sizer without pre-treatment. For subsample two, the ash was chemically pre-treated with 10% HCl before undergoing grain size analysis with laser particle sizer (see Figure S2 in the OSM).

After that, a comparison of the grain size distributions was made.

The ash purification procedure (APP)

We investigated whether the formation of metal oxides and carbonates in a furnace heated to 550°C can impact the accuracy of grain size distribution measurements for the mineral component of biogenic deposits. Therefore, a procedure for purifying the ash from these compounds was proposed. During the study, there was a significant focus on estimating iron oxides FeO and Fe_2O_3, but it is worth noting that ignition can also result in the formation of compounds with other metal elements, such as: K_2O, K_2CO_3, MgO, $MgCO_3$, CaO, $CaCO_3$, Mn_2O_3, Na_2O, Na_2CO_3, ZnO, PbO, CuO, Cu_2O and others.

Metal oxides and carbonates are formed when metal cations (for instance, Fe^{2+}/Fe^{3+}, K^+, Mg^{2+}, Ca^{2+}) contained in organic matter react with carbon dioxide (CO_2) released during ignition, as well as oxygen (O_2) from the surrounding air at high temperatures (Bruchajzer et al. 2017). This reaction follows the equations below:

$$\text{Organic matter} \xrightarrow{T=550℃} CO_2 + Fe^{II} / Fe^{III} \quad (1)$$

$$Fe^{II} / Fe^{III} \xrightarrow{T=550℃;\ O_2} FeO + Fe_2O_3 \quad (2)$$

$$K_2O,\ MgO,\ CaO \xrightarrow{T=550℃;\ CO_2} K_2CO_3,\ MgCO_3,\ CaCO_3 \quad (3)$$

To ensure accurate results of grain size distribution analysis, it is recommended to purify the studied portion of ash containing metal oxides and carbonates using 10% HCl acid (ACS reagent grade). Similar use of acids for the removal of iron oxides was previously described, for example, by Kowalska and Królak (1967) and Surgiewicz (2013). This purification process can prevent the potential impact of aggregates formed by metal compounds on the textural results:

$$FeO + 2HCl \rightarrow Fe^{2+} + 2Cl^- + H_2O \quad (4)$$

$$Fe_2O_3 + 6HCl \rightarrow 2Fe^{3+} + 6Cl^- + 3H_2O \quad (5)$$

$$K_2CO_3 + 2HCl \rightarrow 2K^+ + 2Cl^- + H_2O + CO_2 \uparrow \quad (6)$$

$$MgCO_3 + 2HCl \rightarrow Mg^{2+} + 2Cl^- + H_2O + CO_2 \uparrow \quad (7)$$

$$CaCO_3 + 2HCl \rightarrow Ca^{2+} + 2Cl^- + H_2O + CO_2 \uparrow \quad (8)$$

Here are the steps to apply the ash purification procedure (APP):

1. The ash was mixed in plastic test tubes (for 50 mL) with 30 mL of 10% HCl (the ratio is approximately 1 to 5).
2. The resulting mixture was heated in a water bath to 70°C for 20–30 minutes, and then maintained under regular stirring at a temperature between 70–80°C for 30 minutes (see Figure S3 in the OSM).
3. After the heating process, the test tubes were cooled to room temperature and then subjected to centrifugation for 5 minutes at 4000 rpm. As part of the experiment, the remaining yellowish acid solutions were transferred into separate tubes for spectral analysis (see Figure S4 in the OSM).
4. Following that, the ash underwent 1–2 rounds of centrifugation in distilled water (50 mL) and was subsequently dried at room temperature in the same test tubes. Thus, this procedure effectively purified the ash, removing metal oxides and carbonates, and prepared it for laser textural analysis (Fig. 4).
5. Additionally, we weighed the air-dried ash to two decimal places before and after the ash purification procedure to determine the amount of metal oxides and carbonates removed.

It should be noted that the ash mass measurement before and after the ash purification procedure was conducted following long-term storage of samples at room temperature, which has resulted in moisture inclusion in the ash mass (e.g. see Table S2 in the OSM – Dry ash before/after HCl treatment).

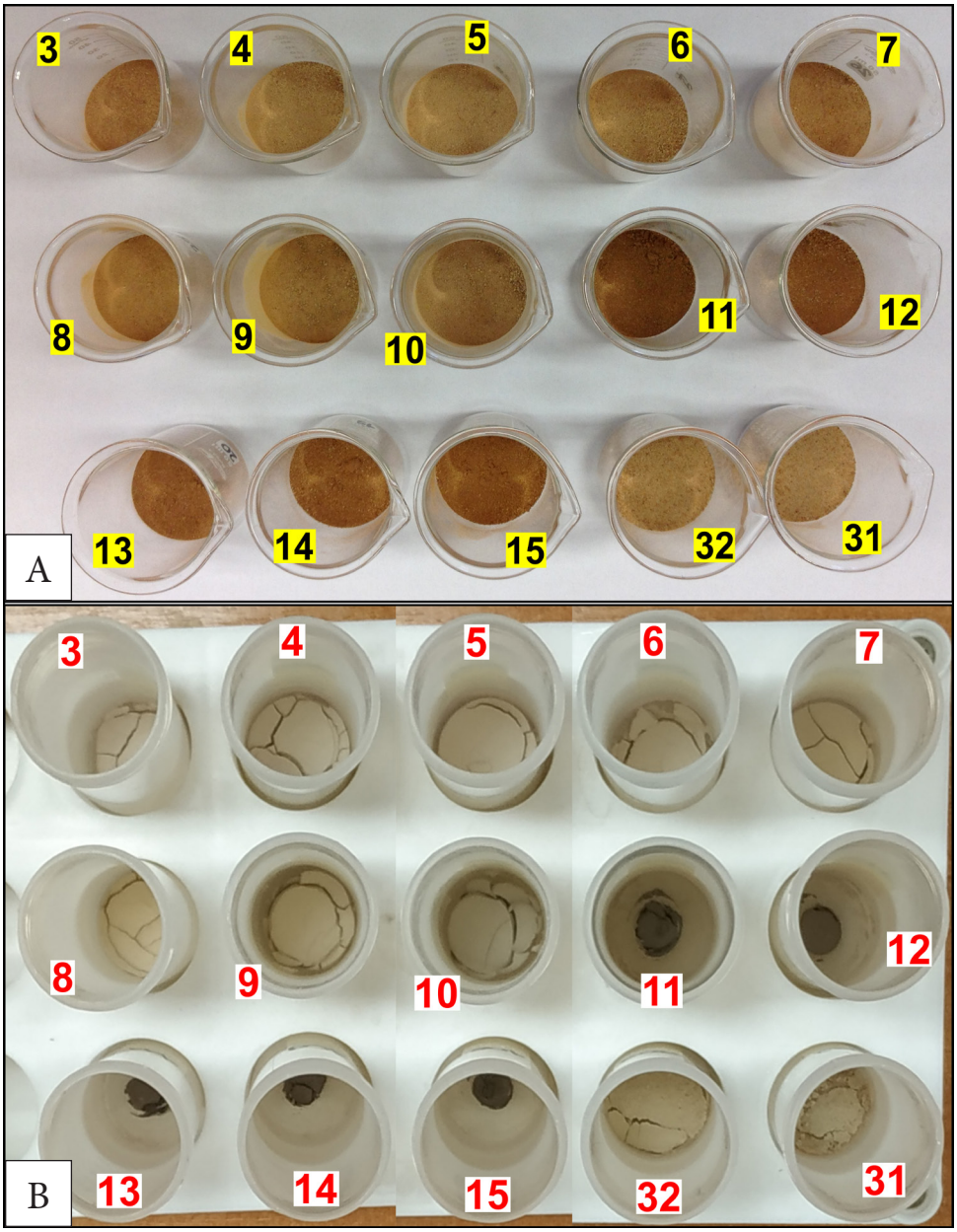

Fig. 4. *View of the studied dry ash before (A) and after (B) the ash purification procedure. The redness has disappeared (photos by D. Tsvirko, 2022)*

Spectral analysis of the HCl acid solutions

After obtaining yellowish acid solutions through APP, 10% HCl was added to each of them up to 50 mL. These solutions were then analyzed using a SPEKOL11 spectrophotometer (on the use of SPEKOL11 see also Tołoczko 2016) to determine the iron content in the ash samples (see Figure S5 in the OSM). To achieve this, eight reference HCl solutions with a known mass and concentration of iron chloride powder ($FeCl_3$) were prepared, each 50 mL in quantity (see Figure S6 in the OSM).

The transmission (T) of each reference solution was measured at wavelengths of 420, 460 and 500 nm. To ensure accuracy, each reference sample underwent five repeated transmission measurements, averaging for each wavelength (Table 1). The relationship between transmission and the mass of iron in solution at wavelengths of 420, 460, and 500 nm are given in Figures S7–S9 in the OSM.

Table 1
Mass and molar concentration of iron in reference samples I–VIII and corresponding average transmission values for wavelengths of 420, 460, and 500 nm

Reference sample number	Mass of Fe in 50 mL of HCl solution [mg]	Molar concentration [mol/dm^3]	*T* (transmission)		
			420 nm	460 nm	500 nm
I	344.276	0.1233000	0.10	0.10	**24.64**
II	172.138	0.0616500	0.10	0.30	**48.12**
III	86.069	0.0308240	0.22	**2.96**	**67.94**
IV	34.428	0.0123300	0.34	**22.48**	**86.54**
V	17.214	0.0061650	**1.14**	**46.50**	91.04
VI	6.886	0.0024660	**13.52**	**70.64**	92.64
VII	3.443	0.0012330	**35.50**	83.48	95.66
VIII	1.721	0.0006165	**57.74**	89.84	96.22

Explanations: values in bold were used to create the graphs in Figures S7–S9 in the OSM.

To determine the mass of iron present in the studied solutions post APP, the transmission (*T*) for each sample was measured using a spectrophotometer. Subsequently, the achieved mass of iron in 50 mL of HCl solution was calculated using the given formulas:

$$\text{For 420 nm, } x = \frac{\ln(83.983)}{0.2516} - \frac{\ln(T)}{0.2516} \quad (9)$$

$$\text{For 460 nm, } x = \frac{\ln(91.881)}{0.04002} - \frac{\ln(T)}{0.04002} \quad (10)$$

$$\text{For 500 nm, } x = \frac{\ln(97.425)}{0.004018} - \frac{\ln(T)}{0.004018} \quad (11)$$

where x – mass of iron in the studied 50 mL of HCl solution [mg], T – transmission of the studied 50 mL of HCl solution.

Atomic absorption spectroscopy (AAS)

After conducting analysis on SPEKOL11 equipment, four acid solutions obtained from APP (samples nos. 3, 4, 11 and 15) were analysed using a Solaar 969 Unicam device (on the use of this device see also Okupny et al. 2020, 2022) for AAS. Through atomic absorption spectrometry, it was possible to identify the presence of other metals aside from iron in post APP solutions.

The main purpose of the analysis using AAS was the qualitative determination of metals present in HCl solutions. For this reason, we decided to analyse only four HCl solutions.

Laser textural analysis

Both ash sample sets (HCl-treated and untreated) were analyzed with a Malvern Panalytical Mastersizer 3000 (see Figure S10 in the OSM), after careful grinding in a porcelain mortar and ultrasonic treatment for 2 minutes in an Ultrasonic Processor Sonicator VCX 130 (see Figure S11 in the OSM). There was no sieving of the samples, since the size of all mineral particles was less than 2 mm.

The grain size distribution results were obtained by statistical processing the initial grain size distribution data using Gradistat Version 9.1 software (Blott & Pye 2001). This initial grain size distribution data included textural results for both untreated and HCl-treated ash, measured on a scale of 1/4 phi. The textural fractions were defined after Udden (1914) and Wentworth (1922) given in micrometres [μm]: coarse sand ($500 \le x < 1{,}000$), medium sand ($250 \le x < 500$), fine sand ($125 \le x < 250$), very fine sand ($63 \le x < 125$), very coarse silt ($31 \le x < 63$), coarse silt ($16 \le x < 31$), medium silt ($8 \le x < 16$), fine silt ($4 \le x < 8$), very fine silt ($2 \le x < 4$) and clay (<2).

To compare two values, we calculated the percentage difference between them using the Formula (12). This was done for mean grain size M_z

values after Folk and Ward (1957) and the textural groups values.

$$x = \frac{A - B}{B} \cdot 100\ \% \tag{12}$$

where: x – percentage difference between two M_z or textural groups values of one sample [%], A – higher M_z or textural group value, B – lower M_z or textural group value.

To estimate the actual organic matter content (OMC after APP) in the samples, excluding metal oxides and carbonates formed during ignition, we used the following formulas:

$$M_{8h\_HCl} = M_{8h} - \frac{M_{8h} \cdot P_r}{100} \tag{13}$$

where: M_{8h_HCl} – ash mass immediately after the muffle furnace, without metal oxides and carbonates [g], M_{8h} – ash mass immediately after the muffle furnace [g] (see Table S1 in the OSM), P_r – the percentage decrease in ash mass after undergoing APP, calculated by comparing the mass of ash (at room temperature) before and after HCl treatment [%] (see Table 2).

$$\text{OMC after APP} = 100 - \frac{M_{8h\_HCl} \cdot 100}{M_s} \tag{14}$$

where: OMC after APP – organic matter content (OMC) after purifying the studied ash from metal oxides and carbonates using APP [%], M_{8h_HCl} – ash mass immediately after the muffle furnace, without metal oxides and carbonates [g], M_s – mass of the entire sample (with organic and mineral components) before ignition [g] (see Table S1 in the OSM).

Microscopic analysis

During the study, we obtained photographs of untreated and HCl-treated ash using a light microscope. Some finds discovered during microscopic analysis of the ash were identified and documented.

RESULTS

HCl treatment results

For the fifteen ash subsamples in the study, the ash purification procedure (APP) was used twice. We recommend performing APP multiple times if redness remains in the ash and the acid solution has a deep yellow color (as per points 1–3 of APP, until the acid solution becomes transparent, see Figure S4B in the OSM).

The purification process effectively removed metal oxides and carbonates from the ash and led to a weight reduction from 6.45 to 72.62% for biogenic deposits and up to 1% for inorganic deposits (Table 2).

For samples with a high content of organic matter such as samples nos. 11–15, there was a noticeable decrease in ash mass of over 50%. During the interaction of ash samples nos. 11–15 with HCl, there was a violent reaction, resulting in the release of CO_2. This reaction may indicate a large amount of metal carbonates formed during LOI_{550} procedure. Other samples with lower LOI_{550} values did not show any reaction with CO_2 release or had minor CO_2 emissions (as sample no. 10). It should be noted that CO_2 emissions only occurred during HCl reaction with ash. Pre-check of samples nos. 10–12 and 14 before the process of ignition showed that there was no reaction between HCl and biogenic samples. This suggests that carbonates were specifically formed during the ignition of biogenic samples in a muffle furnace (LOI_{550} procedure).

Also, for the studied samples, we calculated the actual OMC (Fig. 5) by using the percentage values by which the ash mass decreased after the ash purification procedure (Table 2 – P_r), as per Formulas (13) and (14). The data required for this are presented in Table S1 in the OSM.

Spectral analysis results

Through spectral analysis using the SPEKOL11 equipment, we were able to estimate the initial amount of iron and its oxides present in the ash before chemical treatment. The results from the transmission measurement were used to determine the mass of iron in the yellowish solutions obtained after APP, which are presented in Table 3. In our study, only the acid solutions obtained after a single application of APP on the ash were analysed. As a result, we estimated the amount of iron in the ash based on these solutions, but it is possible that more iron could be present. A small amount of iron might be present in the solutions also after the second application of APP.

Table 2
The studied ash samples and their mass reduction after APP

Sample number	Sample depth [cm]	LOI_{550} [%]	Masses at room temperature		Mass loss (P_r) [%]	Lithological unit	Remarks
			Dry ash before HCl treatment [g]	Dry ash after HCl treatment [g]			
3	10–15	50.940	1.15	0.95	17.39	Brown telmatic peat	No visible CO_2 emission during the reaction of ash with HCl
4	15–20	41.494	1.68	1.48	11.90		
5	20–23	35.921	1.56	1.40	10.26		
6	23–28	31.313	1.22	1.08	11.48		
7	28–33	23.163	2.43	2.22	8.64	Black telmatic peat	
8	33–35	14.790	2.48	2.32	6.45		
9	35–40	29.797	1.56	1.36	12.82		
10	40–45	57.714	1.60	1.20	25.00		Some minor CO_2 emission visible during the reaction of ash with HCl
11	45–49	83.088	0.84	0.23	72.62	Coarse detritus gyttja	Strong CO_2 emission visible during the reaction of ash with HCl
12	49–55	82.766	0.82	0.31	62.20		
13	55–60	81.286	0.88	0.43	51.14		
14	60–65	83.588	0.57	0.24	57.89		
15	65–70	84.611	0.34	0.10	70.59		
31	142–146	5.958	5.97	5.91	1.01	Fine-medium sand	No visible CO_2 emission during the reaction of ash with HCl
32	146–150	3.715	5.92	5.89	0.51		

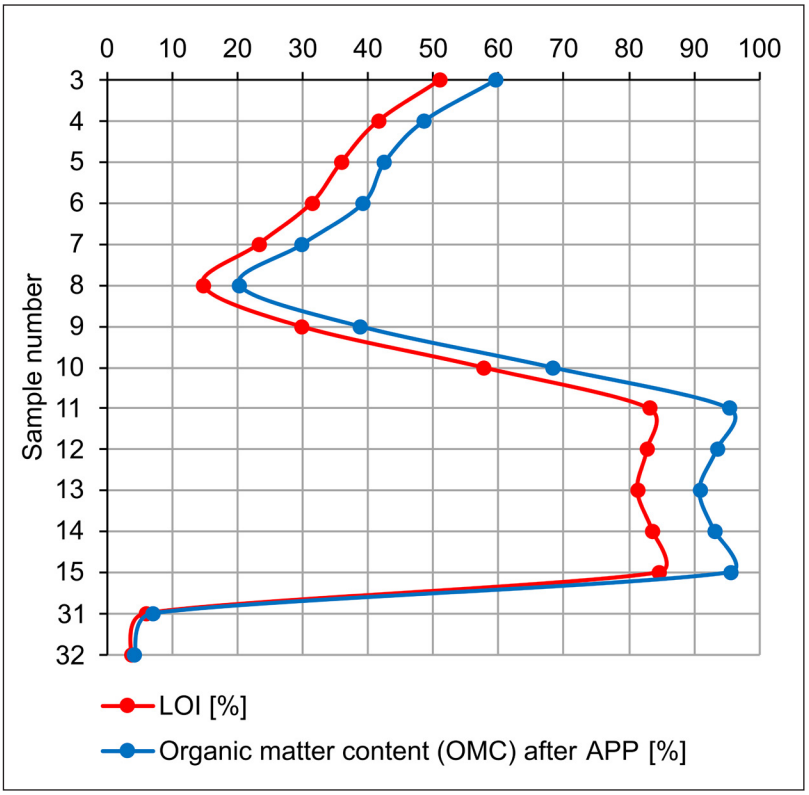

Fig. 5. *The LOI_{550} values in comparison to the organic matter content (OMC) after purifying the studied ash of metal oxides and carbonates using APP*

To compare the results, we also calculated the mass of iron in 300 mg of the ash (Table 3; 300 mg is the smallest mass of ash sample used for the experiment). It can be concluded that the ash from highly organic samples nos. 11–15 and with LOI_{550} values >80% had the largest content of iron (Fig. 6). As expected, the samples with the highest weight loss after APP corresponded to the ones with the largest content of iron and, accordingly, its oxides (samples nos. 11–15).

Table 3

Transmission values, corresponding masses of iron in the solutions after a single use of APP, corresponding amount of iron oxides present in the ash before APP, and iron content in 300 mg of the studied ash

Sample number	*T* (transmission)			Mass of Fe in 50 mL of HCl solution [mg]	Corresponding mass in the ash before APP [mg]		Mass of Fe in 300 mg of ash used for APP (*RT*) [mg]
	420 nm	460 nm	500 nm		Fe_2O_3	FeO	
3	0.3	**19.0**	81.3	39.382	56.306	50.664	10.273
4	0.3	**15.8**	84.0	43.990	62.895	56.593	7.855
5	0.3	**26.3**	86.1	31.258	44.690	40.213	6.011
6	0.4	**33.6**	91.0	25.137	35.939	32.338	6.181
7	0.3	**18.3**	85.3	40.320	57.647	51.871	4.978
8	0.3	**24.7**	85.4	32.826	46.933	42.230	3.971
9	0.3	**23.3**	88.0	34.284	49.017	44.106	6.593
10	0.3	**12.4**	81.2	50.045	71.551	64.383	9.383
11	0.3	2.8	**69.7**	83.346	119.163	107.224	29.766
12	0.3	**4.5**	73.1	75.373	107.764	96.967	27.575
13	0.3	**8.0**	78.9	60.996	87.208	78.471	20.794
14	0.3	**13.4**	83.1	48.107	68.781	61.889	25.319
15	0.3	**24.3**	86.5	33.234	47.516	42.755	29.324
31	8.6	**70.2**	97.4	6.725	9.615	8.652	0.338
32	**12.8**	74.4	98.8	7.477	10.690	9.619	0.379

Explanations: values in bold were used to calculate the masses; *RT* – mass at room temperature.

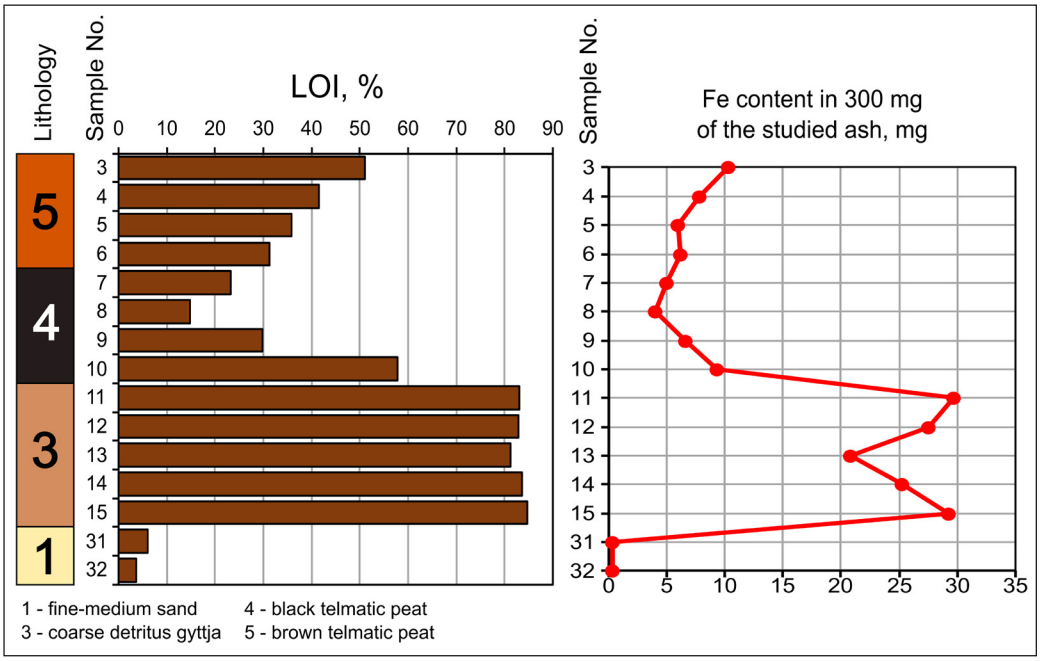

Fig. 6. *The mass of iron present in 300 mg of the ash being studied. Based on spectral analysis of the solutions obtained after a single application of APP and on initial masses of ash used for APP at room temperature*

Atomic absorption spectroscopy (AAS) results

Four HCl solutions (samples nos. 3, 4, 11 and 15) were subjected to AAS to identify the metal elements present. The solutions were found to contain iron (Fe), potassium (K), magnesium (Mg), calcium (Ca), manganese (Mn), sodium (Na), zinc (Zn), lead (Pb) and copper (Cu), with iron being the most dominant.

Textural analysis results

Laser grain size distribution for both untreated and HCl-treated ash are shown in Figures 7 and 8.

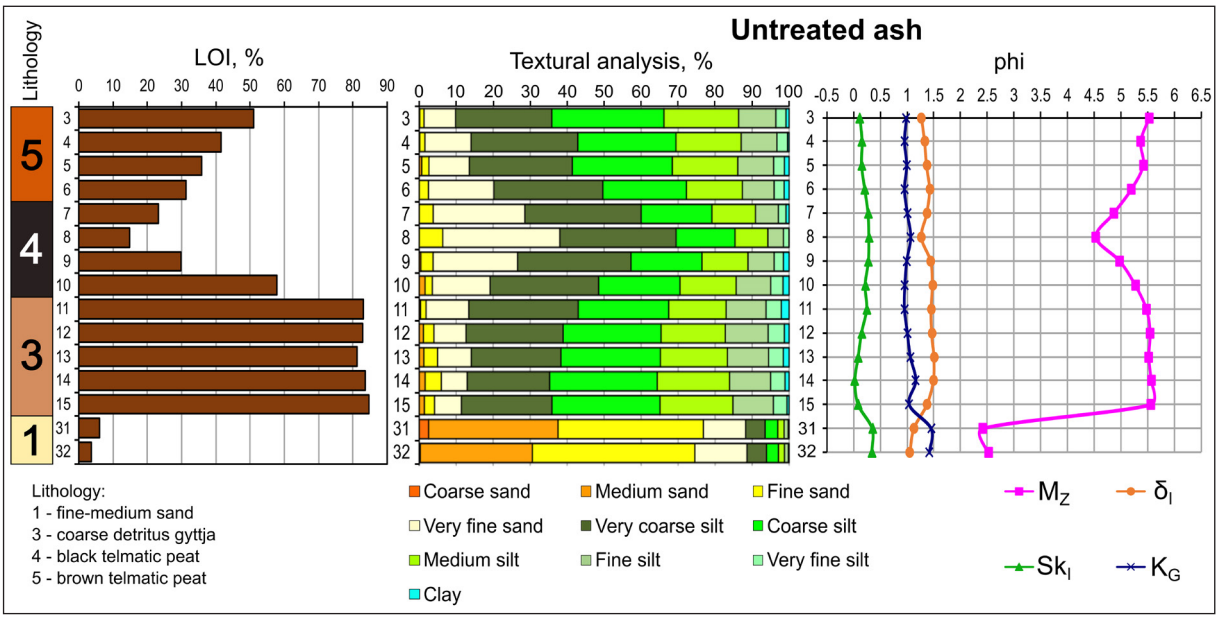

Fig. 7. *Laser grain size distribution for untreated ash*

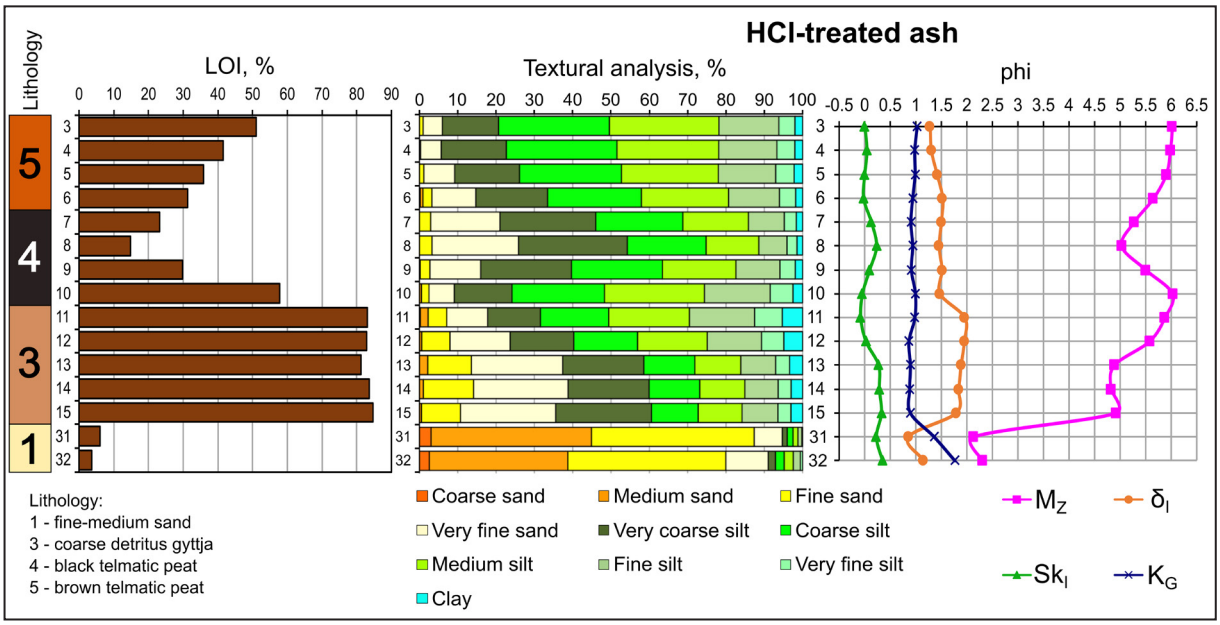

Fig. 8. *Laser grain size distribution for HCl-treated ash*

The results of calculating the mean grain size M_z (using Gradistat software) for the initial grain size distribution data, including the percentage difference in M_z values are shown in Table 4.

Table 4
The mean grain size M_z values for the initial grain size distribution data, along with their percentage differences (after Folk & Ward 1957)

Sample number	Mean grain size (M_z) [µm]		Difference by treatment [%]	Group of samples
	Untreated ash	HCl-treated ash		
3	21.62	15.36	41	I
4	24.18	15.78	53	
5	23.43	16.71	40	
10	25.98	15.35	69	
6	27.31	19.85	38	II
7	34.28	25.85	33	
8	43.23	30.57	41	
9	31.75	22.00	44	
11	22.49	16.99	32	III
12	21.41	20.98	2	
13	21.79	33.75	55	IV
14	21.15	35.33	67	
15	21.30	33.05	55	
31	188.20	227.71	21	V
32	174.64	201.33	15	

After analyzing the data, it was observed that both the untreated and HCl-treated ash samples can be categorized into various groups based on their features (Table 4 – Group of samples). The classification of these groups was determined based on the difference in the LOI_{550} values (Table 2), mean grain size M_z values (Table 4) and on the difference in the textural groups values that were obtained through statistical processing using the Gradistat software (Tables 5, 6).

The first group, consisting of samples nos. 3–5 and 10 (Table 5), showed a relatively large difference in mean grain size (M_z) values (40–70%, Table 4) and LOI_{550} ranging from 35 to 58%. Based on the results of the textural analysis of the ash after APP, this was a group of samples with a low sand content (5.68–9.19%, $M_z \approx 6$ phi). However, the untreated ash samples had a higher amount of sand fraction ranging from 9.83 to 19.19% (M_z = 5.3–5.5 phi). This group of samples had fewer admixture of medium, fine, and very fine silt particles in the untreated ash compared to the HCl-treated ash. Additionally, there was a significant difference in the amount of very coarse silt, with the untreated ash samples containing from 26.03 to 29.33% and the acid treated ash samples containing from 14.68 to 16.99%.

In the second group of samples, which included samples nos. 6–9 (Table 5), the LOI_{550} values ranged from 14 to 32%. The difference in the mean grain size M_z values was around 30–40% (Table 4). The LOI_{550} showed a trend of decreasing and then increasing values. An interesting observation was that the grain size distribution for both untreated and HCl-treated ash samples showed a clear wavy pattern of increase and then decrease of sand fraction (Figs. 7, 8). This means that the textural features were preserved regardless of the state of the ash, with the main difference being the amount of sand fraction. The untreated ash contained more sand (ranging 20.18–38.02%) compared to the samples treated with HCl (ranging 14.72–25.85%). Additionally, the untreated ash had a lower amount of medium, fine, and very fine silts compared to the HCl-treated ash but had a higher amount of very coarse silt.

The third group of samples (nos. 11, 12) showed similarities to the group IV, with LOI_{550} values exceeding 80% (Tables 2, 6). The difference in the mean grain size M_z values was one of the lowest and reached 2% for sample no. 12 and 32% for sample no. 11 (Table 4). This group was notable for its substantial clay admixture in the ash samples after the ash purification procedure (M_z = 5.6–5.9 phi). Additionally, there was a higher percentage of sand fraction present in the ash samples after HCl treatment (17.8 and 23.65%) compared to the untreated samples (12.66 and 13.41%). The untreated ash also had a higher admixture of very coarse silt (26.25 and 29.58%) than the HCl-treated ash (13.76 and 16.64%). Furthermore, there was a higher percentage of coarse silt in the untreated ash compared to the ash after the HCl procedure.

Table 5

Grain size distribution in percentage for Groups I and II, with the percentage difference for the untreated and HCl-treated ash results

Group I	Sample 3			Sample 4			Sample 5			Sample 10		
	Untreated ash [%]	HCl-treated ash [%]	Difference by treatment [%]	Untreated ash [%]	HCl-treated ash [%]	Difference by treatment [%]	Untreated ash [%]	HCl-treated ash [%]	Difference by treatment [%]	Untreated ash [%]	HCl-treated ash [%]	Difference by treatment [%]
Coarse sand	0.00	0.00	–	0.00	0.00	–	0.00	0.00	–	0.01	0.00	–
Medium sand	0.13	0.00	–	0.12	0.00	–	0.67	0.00	–	1.58	0.53	198
Fine sand	1.18	0.95	24	1.44	0.29	397	1.95	1.15	70	1.95	1.95	0
Very fine sand	8.52	5.02	70	12.45	5.39	131	10.92	8.04	36	15.65	6.61	137
Very coarse silt	26.03	14.68	**77**	28.87	16.99	**70**	27.86	16.93	**65**	29.33	15.04	**95**
Coarse silt	30.31	28.93	5	26.55	28.86	9	27.03	26.61	2	22.00	24.15	10
Medium silt	20.18	28.58	**42**	17.60	26.56	**51**	17.69	25.28	**43**	15.18	26.07	**72**
Fine silt	10.07	15.65	**55**	9.67	15.21	**57**	9.70	14.97	**54**	9.35	17.17	**84**
Very fine silt	2.74	4.20	**53**	2.88	4.68	**63**	2.91	4.80	**65**	3.32	5.97	**80**
Clay	0.85	2.00	135	0.43	2.02	374	1.27	2.22	75	1.64	2.50	53
SAND	9.83	5.97	**65**	14.01	5.68	**147**	13.54	9.19	**47**	19.19	9.09	**111**
MUD	90.17	94.03	4	85.99	94.32	10	86.46	90.81	5	80.81	90.91	12
Group II	**Sample 6**			**Sample 7**			**Sample 8**			**Sample 9**		
	Untreated ash [%]	HCl-treated ash [%]	Difference by treatment [%]	Untreated ash [%]	HCl-treated ash [%]	Difference by treatment [%]	Untreated ash [%]	HCl-treated ash [%]	Difference by treatment [%]	Untreated ash [%]	HCl-treated ash [%]	Difference by treatment [%]
Coarse sand	0.00	0.20	–	0.00	0.00	–	0.00	0.00	–	0.00	0.00	–
Medium sand	0.00	0.70	–	0.00	0.00	–	0.00	0.00	–	0.46	0.20	130
Fine sand	2.51	2.35	7	3.78	2.94	29	6.38	3.28	95	3.30	2.52	31
Very fine sand	17.67	11.47	54	24.79	18.07	37	31.64	22.57	40	22.83	13.27	72
Very coarse silt	29.48	18.72	**57**	31.44	24.98	**26**	31.42	28.39	**11**	30.65	23.69	**29**
Coarse silt	22.60	24.49	8	19.14	22.75	19	15.92	20.56	29	19.21	23.73	24
Medium silt	15.12	22.75	**50**	11.76	17.11	**46**	8.90	13.76	**55**	12.43	19.19	**54**
Fine silt	8.56	13.27	**55**	6.18	9.36	**51**	4.20	7.36	**75**	7.07	11.48	**62**
Very fine silt	2.71	4.25	**57**	2.07	3.15	**53**	1.49	2.61	**75**	2.51	4.00	**60**
Clay	1.34	1.80	34	0.85	1.63	91	0.04	1.46	3175	1.55	1.92	24
SAND	20.18	14.72	**37**	28.57	21.01	**36**	38.02	25.85	**47**	26.59	15.99	**66**
MUD	79.82	85.28	7	71.43	78.99	11	61.98	74.15	20	73.41	84.01	14

Explanations: significant differences (in our opinion) are highlighted in bold; SAND – sum of sand fractions; MUD – sum of silt and clay fractions.

Table 6

Grain size distribution in percentage for Groups III, IV and V, with the percentage difference for the untreated and HCl-treated ash results

Group III	Sample 11			Sample 12		
	Untreated ash [%]	HCl-treated ash [%]	Difference by treatment [%]	Untreated ash [%]	HCl-treated ash [%]	Difference by treatment [%]
Coarse sand	0.00	0.23	–	0.00	0.00	–
Medium sand	0.36	2.03	463	1.12	0.59	91
Fine sand	1.50	4.88	**225**	2.86	7.39	**158**
Very fine sand	11.55	10.67	8	8.68	15.68	81
Very coarse silt	29.58	13.76	**115**	26.25	16.64	**58**
Coarse silt	24.49	17.82	**37**	26.48	16.64	**59**
Medium silt	15.50	21.09	36	17.35	18.18	5
Fine silt	10.78	17.00	58	11.58	14.17	22
Very fine silt	4.13	7.23	75	4.39	5.83	33
Clay	2.11	5.30	**151**	1.28	4.90	**282**
SAND	13.41	17.80	**33**	12.66	23.65	**87**
MUD	86.59	82.20	5	87.34	76.35	14

Group IV	Sample 13			Sample 14			Sample 15		
	Untreated ash [%]	HCl-treated ash [%]	Difference by treatment [%]	Untreated ash [%]	HCl-treated ash [%]	Difference by treatment [%]	Untreated ash [%]	HCl-treated ash [%]	Difference by treatment [%]
Coarse sand	0.00	0.01	–	0.00	0.00	–	0.00	0.00	–
Medium sand	1.26	2.16	71	1.60	1.02	58	1.41	0.53	166
Fine sand	3.70	11.41	**208**	4.39	13.12	**199**	2.73	10.18	**273**
Very fine sand	9.10	23.82	**162**	6.98	24.66	**253**	7.29	24.86	**241**
Very coarse silt	24.26	21.16	15	22.30	21.14	5	24.46	24.97	2
Coarse silt	26.89	13.32	**102**	29.07	13.21	**120**	29.22	12.20	**139**
Medium silt	18.13	11.99	51	19.57	11.78	66	19.70	11.43	72
Fine silt	11.14	9.10	22	11.10	8.70	28	10.91	9.37	16
Very fine silt	3.95	3.64	9	3.89	3.38	15	3.71	3.41	9
Clay	1.58	3.40	**115**	1.10	3.00	**172**	0.57	3.04	**431**
SAND	14.06	37.38	**166**	12.97	38.79	**199**	11.43	35.57	**211**
MUD	85.94	62.62	37	87.03	61.21	42	88.57	64.43	37

Group V	Sample 31			Sample 32		
	Untreated ash [%]	HCl-treated ash [%]	Difference by treatment [%]	Untreated ash [%]	HCl-treated ash [%]	Difference by treatment [%]
Coarse sand	2.55	3.02	18	0.29	2.57	786
Medium sand	34.98	41.87	20	30.30	36.14	19
Fine sand	39.31	42.47	8	43.93	41.24	7
Very fine sand	11.40	7.34	55	14.10	11.07	27
Very coarse silt	5.27	1.29	**308**	5.29	1.90	**178**
Coarse silt	3.43	1.51	**127**	3.20	2.26	**41**
Medium silt	1.70	1.26	34	1.63	2.37	46
Fine silt	1.10	1.05	5	1.06	1.85	74
Very fine silt	0.26	0.18	44	0.20	0.59	194
Clay	0.00	0.00	–	0.00	0.00	–
SAND	88.24	94.70	7	88.62	91.02	3
MUD	11.76	5.30	**122**	11.38	8.98	**27**

Explanations: significant differences (in our opinion) are highlighted in bold; SAND – sum of sand fractions; MUD – sum of silt and clay fractions.

The fourth group is represented by samples nos. 13–15 (Table 6) with LOI_{550} values above 80%. The difference in the mean grain size M_z values was around 55–65% (Table 4). This group showed significant differences in the results of grain size distribution between samples of untreated and HCl treated ash. The amount of sand fraction in the analyzed samples was notably different, with HCl-treated ash having higher sand fraction admixture (over 35% of sands, and $M_z \approx 5$ phi) compared to untreated ash (less than 15%, and $M_z \approx 5.5$ phi respectively). Additionally, the ash samples from this group have more clay fraction after HCl treatment, while untreated ash showed a higher amount of coarse silt fraction (up to 30%).

The fifth group consisted of sand samples nos. 31 and 32 (Table 6) with LOI_{550} values <6%. This group had a difference in the mean grain size M_z values of about 15–20%. Notably, the untreated ash had a more significant amount of silt fraction (11.38 and 11.76% in samples nos. 32 and 31, respectively) compared to the ash treated with HCl (5.3 and 8.98%). As a result, the mean grain size in phi scale (M_z) for the samples after APP was lower (with values tending towards 2 phi) than for the untreated ash samples (about 2.5 phi). The main difference among the silt fractions was the higher quantity of very coarse and coarse silts in the untreated ash samples (8.49 and 8.7%) compared to the HCl-treated samples (2.8 and 4.16%).

Microscopic analysis results

The results of the analysis of untreated and HCl-treated ash under a light microscope are presented in Figure 9.

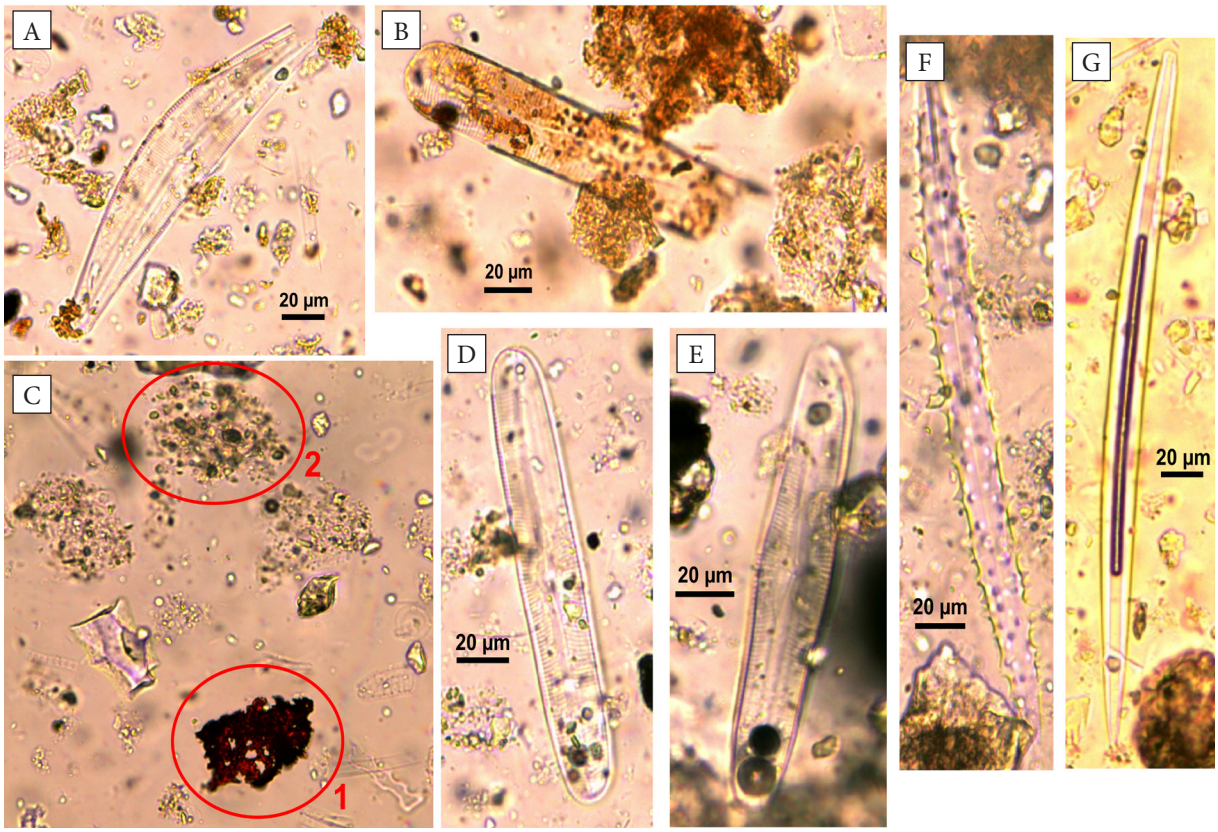

Fig. 9. *Microscopic images of individual components of the studied ash from the core PKK-1-2 (photos by D. Tsvirko, 2023): A), B) diatoms Cymbella sp. (A) and Pinnularia sp. (B) from the untreated ash sample no. 3 (depth: 10–15 cm); C) HCl-treated ash sample no. 3 (depth: 10–15 cm) with a fragment of mineral particles probably bonded by metal compounds (1) and a fragment of mineral particles separated from metal compounds by APP (2), the photo without a scale bar; D), E) diatoms Pinnularia sp. from the HCl-treated ash sample no. 3 (depth: 10–15 cm); F), G) freshwater sponge spicules in the HCl-treated ash sample no. 4 (depth: 15–20 cm)*

DISCUSSION AND INTERPRETATION

Ash mass loss after HCl treatment

After undergoing the ash purification procedure (APP), the ash being studied experienced a decrease in weight (Table 2). Spectral analysis revealed that this weight loss was partly due to the removal of iron compounds from the ash (Table 3), including iron oxides that had been formed during ignition in a muffle furnace (during LOI_{550} procedure). Since before APP iron was in the form of oxides, the masses of these compounds were estimated using data from the SPEKOL11 spectral analysis (Table 3). The masses of iron oxides FeO and Fe_2O_3 were calculated based on the total mass of Fe found in the acid solution, and represented the maximum possible mass of iron oxide (FeO or Fe_2O_3) present in the ash sample (Table 3). However, it is most likely that part of the Fe was in the form of FeO, while the other part was in the form of Fe_2O_3.

If we compare the masses of iron oxides listed in Table 3 with the amount of disappeared ash at room temperature (Table 2), it becomes clear that the iron compounds did not occupy the entire size of the disappeared mass, but only part of it: Fe_2O_3 could potentially occupy from 16.03 to 35.63% of the disappeared mass, while FeO – from 14.42 to 32.06%. However, it should be noted that the percentage comparison provided was based on the mass at room temperature, and did not account for moisture absorbed by the ash. In our study, we did not use a desiccator, so moisture from the air at room temperature was included in the ash mass. In fact, it is important to consider that a greater volume of ash was occupied by iron oxides.

According to atomic absorption spectrometry results, the rest of the disappeared mass was likely constituted by other metal compounds such as K_2O, K_2CO_3, MgO, $MgCO_3$, CaO, $CaCO_3$, MnO_2, Na_2O, Na_2CO_3, ZnO, PbO, CuO, Cu_2O and others.

Environmental factors and metal content in biogenic deposits

The ash purification procedure resulted in the highest ash weight loss (ranging from 51.14 to 72.62% – Table 2) for samples nos. 11–15 which had LOI_{550} values between 80 and 85%. These samples were highly organic, which apparently contributed to their ability to absorb a greater amount of metal elements from the environment (on metal absorption see Rashid 1974, Brown et al. 2000, Krumins & Robalds 2015). For instance, the significant presence of Fe in samples nos. 11–15 (Fig. 6) could be due to its absorption from iron-saturated groundwater (on groundwater fluctuations and Fe see Bigham et al. 2002). However, it cannot be concluded that samples rich in organic always contain a substantial amount of absorbed metal compounds. Additional experiments on other highly organic samples, such as samples nos. 19–24 and 28 (with LOI_{550} values ranging 69.33–76.42% – Table S2 in the OSM, Fig. 3), showed that the ash mass loss after the APP and the amount of metal elements and their oxides and carbonates were not as significant as for samples nos. 11–15. In this case, it is more appropriate to refer to the potential of a large amount of organic matter to absorb more metal elements from the environment.

It is important to consider that other environmental factors can impact the metal content in organic matter. Specifically, high levels of Fe observed in samples nos. 11–15 and additional samples nos. 16–18 (Fig. 3, Table S2 in the OSM) may be attributed to fluctuations in the level of groundwater saturated with Fe (on this topic see Bigham et al. 2002). During the profile sampling in August 2020, the groundwater level was at approximately 0.8 m below surface – which aligns with the range of these samples. We believe that in our case, the fluctuations in groundwater level were the key determinant in the distribution of metals compounds in the sediment profile.

In fact, metal cations, which were part of oxides and carbonates, may accumulate in biogenic deposits through various means. Groundwater saturated with metal elements has been identified as one possible source (on this topic see Bigham et al. 2002). Metal accumulation in living organisms during their vital activities is another potential source, especially for plant organisms that are fundamental in the formation of biogenic deposits. Plants require elements such as Fe, K, Mn, Na, Zn, Cu, and others to survive and develop (Vatansever et al. 2017, Kaur et al. 2023). One more possible source is metal contamination of biogenic deposits and plants as a result of anthropogenic activities (Patel et al. 2020). However, the APP described in this study effectively removed all these

metals from the ash. The authors suggest that these metal cations should be considered either as part of the organic component of biogenic sediments or as part of post-sedimentary processes (i.e. formation of metal compounds as a result of fluctuations in the groundwater level, natural decomposition, and the humification of organic matter, etc.). To avoid misinterpretations of the textural analysis results, it is necessary to remove these metal cations from the ash.

Actual organic matter content (OMC) in geological deposits

After removing both metal cations and their oxides and carbonates from the ash samples, we were able to estimate the actual OMC (Fig. 5). In fact, biogenic deposits had more organic matter than what was initially shown through the LOI_{550} method, which does not account for the formation of metal oxides and carbonates during the ignition process. When considering metal cations as part of the mineral component of biogenic sediments, the actual organic matter content will lie between the LOI_{550} values and the values of OMC after APP (Fig. 5).

Use of the ash for laser textural analysis

By applying the proposed procedure of using HCl acid to purify ash from metal oxides and carbonates, we gained insights into the problem of using the ash for textural analysis.

Based on our investigations, it has been established that relying on results of textural analysis for untreated ash from organic samples with LOI_{550} values exceeding 80% can lead to inaccurate interpretations. For instance, our analysis showed that untreated ash samples nos. 13–15 did not reflect the substantial sand fraction admixture as recorded after APP (Figs. 7, 8). Moreover, the results for untreated ash of highly organic samples nos. 11 and 12 did not mirror the actual grain size distribution. From the diagram presented in Figure 7, it is evident that the untreated ash samples nos. 11 and 12 had a sand fraction content that was nearly identical to samples nos. 13–15. However, upon analyzing the HCl-treated ash, it was revealed that the sand fraction admixture in samples nos. 11 and 12 was significantly lower (Fig. 8). It should also be noted that the untreated ash for samples nos. 11 and 12 obscured a considerable amount of clay and medium silt fractions in the mixture. All these observations can be explained by the fact that such highly organic deposits, with high admixture of metals (Figs. 3, 6), form high amount of metal oxides and carbonates during ignition in a muffle furnace. Aggregates formed by these metal compounds and silt and clay particles impact on the results of grain size distribution analysis for the mineral component of biogenic deposits (i.e. for ash samples after LOI_{550} procedure).

Among the samples analyzed, the formation of metal carbonates took place almost exclusively in highly organic samples nos. 11–15 (Table 2). The untreated ash from these samples also had the strongest red color (Fig. 4A), but after interacting with HCl, it changed to grey color (Fig. 4B), along with the disappearance of most of the ash mass (Table 2). Accordingly, the amount of organic matter in the samples was an important factor that should be taken into account when planning textural analysis of the ash after LOI_{550}. This is because the more organic matter in sediments, the more CO_2 is released during ignition, which forms carbonates upon further reaction with metal oxides (Formula (3)). Additionally, the more organic matter in the sediments, the more metals can potentially be absorbed from the natural environment, which later form metal oxides and carbonates during ignition, "contaminating" the studied ash for textural analysis. Also, the more organic matter together with metals in the sediments, the greater volume of their ash will contain aggregates of metal oxides and carbonates.

The next detail was that the ash from the samples with lower organic matter content (around 30% or less), formed fewer metal compounds during ignition (Table 2). Our results show that this was the case for samples nos. 6–9, for which LOI_{550} values ranging from 14.79 to 31.31% and a high admixture of sand fraction was defined. This sand admixture was visible both in the results of textural analysis of the untreated ash and the HCl-treated ash (as shown in Figures 7, 8). Therefore, it is generally advisable to rely on the textural analysis data of the untreated ash, but only to observe the granulometric trend of the sand admixture. However, it is important to note that the textural analysis of untreated ash in such cases can only reveal the trend of sand admixture, while

the obtained quantitative values will not necessarily reflect the actual composition of the mineral component of biogenic deposits. The untreated ash samples nos. 6–9 contained significantly more sand-sized particles than the HCl-treated samples.

In our example, we encountered an unclear situation involving medium organic samples (nos. 3–5 and 10). For these samples LOI_{550} values range from 35.92 to 57.71% (Table 2). On the one hand, there seemed to be a slight presence of sand fraction in both the untreated ash and the HCl-treated ash (Figs. 7, 8). The amount of coarse silt was very similar for these samples (Table 5). However, on the other hand, the untreated ash contained more very coarse silt, while the HCl-treated ash had more medium, fine, and very fine silt fractions. To ensure more reliable results for ash textural analysis of medium organic samples, the authors recommend using the APP described in this paper.

During the analysis of sand samples nos. 31 and 32, an interesting discovery was made regarding the "contamination" of untreated ash. It was found that this "contamination" was mainly caused by silt particles. It was especially well seen in the case of untreated ash of sample no. 31 (which had a LOI_{550} of 5.96%), containing twice as much silt (primarily coarse and very coarse silt) as the HCl-treated ash (Table 6). However, overall results indicated that sand samples with minimal organic matter (LOI_{550} values <6%, Table 3) can be analyzed for ash texture without APP treatment. The grain size distribution analysis of both untreated and HCl-treated ash for samples nos. 31 and 32 showed that fine and medium sand fractions were dominant.

Based on the collected materials, we can draw some general conclusions. All untreated ash samples had an excess of very coarse silt or, in some cases, coarse silt when compared to the HCl-treated samples. Accordingly, metal oxides and carbonates formed in the muffle furnace had a significant impact on the amount of these fractions and can obscure the results of grain size distribution analysis. It is possible that metal oxides and carbonates grew on the surface of small silt particles, causing them to enlarge and become coarse and very coarse silts, and sometimes even very fine sand, as noted for samples nos. 3–10, 31 and 32. Metal compounds may have also grown on sand particles, increasing their size. It is also possible that particles stuck together to form aggregates due to the formation of metal oxides and carbonates (Fig. 9C). Further studies and verification are needed to confirm these conclusions about the form of existence of metal compounds at the ash micro level after LOI_{550} procedure.

It is important to note that in samples nos. 11–15, 31 and 32 there was a distinct increase in the amount of sand fraction after HCl treatment (Table 6), which in some cases led to an increase in the mean grain size M_z (samples nos. 13–15, 31 and 32 – Table 4). For samples nos. 11–15, we explain this by a decrease in ash volume after the HCl procedure (Fig. 4). After undergoing HCl treatment, these samples exhibited a significant decrease in the amount of very coarse and coarse silt fractions. This resulted in relative increase of content of sand fraction. Thus, sand fraction constituted a higher proportion of the ash volume after HCl treatment. A decrease in the content of very coarse and coarse silt particles after APP also occurred for samples nos. 31 and 32.

A separate topic for research is how the temperature of 550°C affects the mineral component and whether mineral particles could be destroyed in the muffle furnace. Here we only note that the diatoms found during the microscopic analysis of the studied ash retained their sculpture after heating to 550°C (Fig. 9).

The suggested ash purification procedure (APP) can assist in identifying lithological boundaries when there is uncertainty. This approach is particularly useful in cases like ours, where samples nos. 6–9 showed a considerable sand content that could be indicative of lithological boundaries.

It is important to note, however, that our conclusions were based on a limited selection of samples (only fifteen in total). Nevertheless, the samples we presented were varied in composition and represent diverse deposit types.

CONCLUSIONS

The summary included the following findings from the research:

1. The ash purification procedure (APP) was introduced as a laboratory technique to purify ash from secondary metal oxides and carbonates that are formed during ignition at 550°C with absorption of O_2 and CO_2 from the

atmosphere. The quantity of metal oxides and carbonates in the ash is dependent primarily on the amount of metals found in the biogenic deposits before ignition. All these impurities distort the results of grain size distribution analysis of the untreated ash after LOI_{550} procedure.

2. Following the implementation of the ash purification procedure (APP), there was a decrease in the ash mass as a result of elimination of secondary metal oxides and carbonates. The higher the presence of metal oxides and carbonates in the ash, the more significant the reduction in ash mass.
3. A particularly significant difference between the results of grain size distribution analysis for untreated and HCl-treated ash was documented for highly organic deposit samples containing substantial amounts of metal compounds. To avoid any possible misinterpretations, we recommend that the ash be purified of metal compounds before undergoing textural analysis.
4. According to the obtained results, the untreated ash of all investigated samples was featured by higher amount of very coarse and/or coarse silt fractions compared to the HCl-treated ash. This is due to the formation of aggregates of metal oxides and carbonates with mineral particles during LOI_{550} procedure. Additionally, the untreated ash had a lower content of medium, fine, very fine silt, and/or clay fractions compared to the HCl-treated ash.

We would like to express our gratitude to Dr Artur Ginter for allowing us to utilize the muffle furnace at the Laboratory of Luminescence Dating and Conservation of Artifacts of University of Lodz. Our heartfelt appreciation also goes to Prof. Jacek Szmańda for granting us access to work on the Malvern Panalytical Mastersizer 3000 laser at the Institute of Geography Pedagogical University of Krakow. We are grateful to Dr Tatyana Yakubovskaya for providing data on the analysis of plant macrofossils for the PKK-1-2 core. In addition, we extend our thanks to Dr Daniel Okupny for conducting atomic absorption spectrometry (AAS) at the Institute of Marine and Environmental Sciences of University of Szczecin. Our gratitude is also expressed to Prof. Monika Rzodkiewicz for the identification of diatoms and to Maciej Gałecki for his invaluable assistance with mathematical calculations and formulas. We express our gratitude to the reviewers for providing us with their valuable comments and advice. Lastly, we would like to acknowledge the support provided by the UŁ IDUB grant (Nr decyzji – NR 7/ODW/DGB/2022) for this study.

REFERENCES

Bigham J.M., Fitzpatrick R.W. & Schulze D.G., 2002. Iron Oxides. [in:] Dixon J.B. & Schulze D.G. (Eds.), *Soil Mineralogy with Environmental Applications,* SSSA Book Series, 7, Soil Science Society of America, Madison, 323–366. https://doi.org/10.2136/sssabookser7.c10.

Blott S.J. & Pye K., 2001. GRADISTAT: Agrain size distribution and statistics package for the analysis of unconsolidated sediments. *Earth Surface Processes and Landforms*, 26(11), 1237–1248. https://doi.org/10.1002/esp.261.

Brown P.A., Gill S.A. & Allen S.J., 2000. Metal removal from wastewater using peat. *Water Research*, 34(16), 3907–3916. https://doi.org/10.1016/S0043-1354(00)00152-4.

Bruchajzer E., Frydrych B. & Szymańska J., 2017. Tlenki żelaza – w przeliczeniu na Fe. Dokumentacja proponowanych dopuszczalnych wielkości narażenia zawodowego. *Podstawy i Metody Oceny Środowiska Pracy*, 2(92), 51–87. https://doi.org/10.5604/01.3001.0009.9360.

Dean W.E. Jr., 1974. Determination of carbonate and organic matter in calcareous sediments and sedimentary rocks by loss on ignition: Comparison with other methods. *Journal of Sedimentary Petrology*, 44(1), 242–248. https://doi.org/10.1306/74D729D2-2B21-11D7-8648000102C1865D.

Folk R.L. & Ward W.C., 1957. Brazos River bar: A study in the significance of grain size parameters. *Journal of Sedimentary Petrology*, 27(1), 3–26. https://doi.org/10.1306/74D70646-2B21-11D7-8648000102C1865D.

Heiri O., Lotter A.F. & Lemcke G., 2001. Loss on ignition as a method for estimating organic and carbonate content in sediments: reproducibility and comparability of results. *Journal of Paleolimnology*, 25(1), 101–110. https://doi.org/10.1023/A:1008119611481.

Kaur H., Kaur H., Kaur H. & Srivastava S., 2023. The beneficial roles of trace and ultratrace elements in plants. *Plant Growth Regulation*, 100(2), 219–236. https://doi.org/10.1007/s10725-022-00837-6.

Kissinger H.E., McMurdie H.F. & Simpson B.S., 1956. Thermal decomposition of manganous and ferrous carbonates. *Journal of the American Ceramic Society*, 39(5), 168–172. https://doi.org/10.1111/j.1151-2916.1956.tb15639.x.

Kittel P., Mazurkevich A., Alexandrovskiy A., Dolbunova E., Krupski M., Szmańda J., Stachowicz-Rybka R., Cywa K., Mroczkowska A. & Okupny D., 2020. Lacustrine, fluvial and slope deposits in the wetland shore area in Serteya, Western Russia. *Acta Geographica Lodziensia*, 110, 103–124. https://doi.org/10.26485/AGL/2020/110/7.

Kittel P., Muzolf B., Płóciennik M., Elias S., Brooks S.J., Lutyńska M., Pawłowski D., Stachowicz-Rybka R., Wacnik A., Okupny D., Głąb Z. & Mueller-Bieniek A., 2014. A multi-proxy reconstruction from Lutomiersk-Koziówki, Central Poland, in the context of early modern hemp and flax processing. *Journal of Archaeological Science*, 50, 318–337. https://doi.org/10.1016/j.jas.2014.07.008.

Kittel P., Płóciennik M., Borówka R.K., Okupny D., Pawłowski D., Peyron O., Stachowicz-Rybka R., Obremska M. & Cywa K., 2016. Early Holocene hydrology and environments of the Ner River (Poland). *Quaternary Research*, 85(2), 187–203. https://doi.org/10.1016/j.yqres.2015.12.006.

Kowalska J. & Królak B., 1967. Wybielanie i usuwanie tlenków żelaza z surowców kaolinowych okolic Bolesławca metodami chemicznymi. *Przegląd Geologiczny*, 15(2), 120–121.

Krumins J. & Robalds A., 2015. Biosorption of metallic elements onto fen peat. *Environmental and Climate Technologies*, 14(1), 12–17. https://doi.org/10.1515/rtuect-2014-0008.

Markowski S., 1980. Struktura i właściwości podtorfowych osadów jeziornych rozprzestrzenionych na Pomorzu Zachodnim jako podstawa ich rozpoznawania i klasyfikacji [Structure and properties of peatlands' bottom lake sediments of frequent occurrence in West Pomerania region as a basis for their identification and classification]. [in:] *Krajowa konferencja naukowo techniczna Kreda jeziorna i gytie: Materiały pokonferencyjne: Lubniewice, 8–10 XI 1979 r. Tom 2*, Urząd Wojewódzki w Gorzowie Wielkopolskim, Gorzów Wielkopolski – Zielona Góra, 45–55.

Mikutta R., Kleber M., Kaiser K. & Jahn R., 2005. Review: Organic matter removal from soils using hydrogen peroxide, sodium hypochlorite, and disodium peroxodisulfate. *Soil Science Society of America Journal*, 69(1), 120–135. https://doi.org/10.2136/sssaj2005.0120.

Okupny D., Borówka R.K., Cedro B., Sławińska J., Tomkowiak J., Michczyński A., Kozłowska D., Kowalski K. & Siedlik K., 2020. Geochemistry of a sedimentary section at the Wąwelnica archaeological site, Szczecin Hills (Western Pomerania). *Acta Geographica Lodziensia*, 110, 169–186. https://doi.org/10.26485/AGL/2020/110/11.

Okupny D., Antczak-Orlewska O., Pawłowski D., Borówka R.K., Sławińska J., Tomkowiak J., Osóch P., Bartczak A., Nierychlewska A., Osóch B., Krąpiec M., Jucha W., Kittel P., Sady-Bugajska A. & Spławski S., 2022. How well multi-indicator palaeo-environmental studies meet the needs of research on settlements, on the example of the early medieval settlement complex in Szczecin: methodological problems and evaluating interpretation value. *Acta Geographica Lodziensia*, 112, 97–121. https://doi.org/10.26485/AGL/2022/112/7.

Patel A., Tiwari S., Raju A., Pandey N., Singh M. & Prasad S.M., 2020. Heavy metal contamination of environment and crop plants. [in:] Mishra K., Tandon P.K. & Srivastava S. (eds.), *Sustainable Solutions for Elemental Deficiency and Excess in Crop Plants*, Springer, Singapore, 303–333. https://doi.org/10.1007/978-981-15-8636-1_12.

Rashid M.A., 1974. Absorption of metals on sedimentary and peat humic acids. *Chemical Geology*, 13(2), 115–123. https://doi.org/10.1016/0009-2541(74)90003-5.

Surgiewicz J., 2013. Metoda oznaczania tlenków żelaza na stanowisku pracy. *Podstawy i Metody Oceny Środowiska Pracy*, 1(75), 89–99.

Tobolski K., 2021. *Przewodnik do oznaczania torfów i osadów jeziornych*. Wydawnictwo Naukowe PWN, Warszawa.

Tołoczko W., 2016. Method for determining iodine-127 in soils. *Soil Science Annual*, 67(4), 197–203. https://doi.org/10.1515/ssa-2016-0025.

Tsvirko D., 2023. The natural environment in the vicinity of Lake Sporovskoye in the Late Glacial and Holocene. *Acta Palaeobotanica*, 63(1), 65–86. https://doi.org/10.35535/acpa-2023-0005.

Tsvirko D., Kalicki T. & Trifonov Y., 2021a. The history of the development of the natural environment in the Kokoritsa microregion (Belarus). [in:] *7th International Scientific Conference GEOBALCANICA 2021: Proceedings: 15–16 June 2021, Ohrid, North Macedonia: Hybrid Conference*, Geobalcanica Society, Skopje, 101–110. https://doi.org/10.18509/GBP210101t.

Tsvirko D., Kryvaltsevich M., Tkachou A., Trifonov Y., Kalicki T., Frączek M. & Kusztal P., 2021b. Late Glacial and Holocene evolution of landscapes on the territory of Sporovsky Reserve (Belarusian Polesie). *Acta Geobalcanica*, 7–3, 93–100. https://doi.org/10.18509/AGB.2021.13.

Tsvirko D., Tołoczko W. & Kittel P., 2022a. Sedimentological analysis of the ash remaining after Loss-On-Ignition – methodological aspect. [in:] Dzieduszyńska D. (red.), *Sesja naukowa: Paleogeografia schyłku vistulianu: Popów, 13–14 czerwca 2022 r.*, Katedra Geologii i Geomorfologii Uniwersytetu Łódzkiego, Komitet Badań Czwartorzędu Polskiej Akademii Nauk, Stowarzyszenie Geomorfologów Polskich, Popów, 47–49.

Tsvirko D., Tołoczko W. & Kittel P., 2022b. *Sedimentological analysis of the ash remaining after Loss-On-Ignition – methodological aspect* [poster]. Paleogeografia schyłku Vistulianu, Popów, Poland, 13–14 June 2022. https://www.researchgate.net/publication/361554900_Sedimentological_analysis_of_the_ash_remaining_after_Loss-On-Ignition_-_methodological_aspect_POSTER.

Udden J.A., 1914. Mechanical composition of clastic sediments. *Geological Society of America Bulletin*, 25(1), 655–744. https://doi.org/10.1130/GSAB-25-655.

Vatansever R., Ozyigit I.I. & Filiz E., 2017. Essential and beneficial trace elements in plants, and their transport in roots: A review. *Applied Biochemistry and Biotechnology*, 181(1), 464–482. https://doi.org/10.1007/s12010-016-2224-3.

Wentworth C.K., 1922. A scale of grade and class terms for clastic sediments. *The Journal of Geology*, 30(5), 377–392. https://doi.org/10.1086/622910.

Żarczyński M., Szmańda J. & Tylmann W., 2019. Grain-size distribution and structural characteristics of varved sediments from Lake Żabińskie (Northeastern Poland). *Quaternary*, 2(1), 8. https://doi.org/10.3390/quat2010008.

Supplementary data associated with this article can be found, in the online version, at:
https://doi.org/10.7494/geol.2024.50.2.155